Aptamer-Based Tumor-Targeted Drug Delivery for Photodynamic Therapy

Yen-An Shieh,[†,§] Shu-Jyuan Yang,[†,§] Ming-Feng Wei,[†] and Ming-Jium Shieh[†,‡,*]

[†]Institute of Biomedical Engineering, College of Medicine and College of Engineering, National Taiwan University, Taipei 10051, Taiwan, and [‡]Department of Oncology, National Taiwan University Hospital and College of Medicine, Taipei 10002, Taiwan. [§]These authors contributed equally to this work.

ABSTRACT A specialized G-rich DNA structure, G-quadruplex, has been studied for its special physical characteristics and biological effects. Herein we report a novel strategy of using G-quadruplex as a drug carrier to target cancer cells for photodynamic therapy (PDT). A G-quadruplex forming AS1411 aptamer could be physically conjugated with six molecules of porphyrin derivative, 5,10,15,20-tetrakis(1-methylpyridinium-4-yl)porphyrin (TMPyP4), to fabricate the apt-TMP complex. The TMPyP4 molecules in the complex were identified to bind tightly to the aptamer by intercalation and outside binding. Because the G-quadruplex structure is known to target the overexpressed nucleolin in cancer cells, in this study, the effect of the G-quadruplex structure as a carrier for the delivery of TMPyP4 into cancer cells by nucleolin-mediated internalization was investigated. The results showed that the apt-TMP complex exhibited a higher TMPyP4 accumulation in MCF7 breast cancer cells than in M10 normal epithelium cells. After treated with light for 180 s, the photodamage in MCF7 cells was larger than in M10 cells. These results indicated that the TMPyP4 delivery and uptake were mediated by the specific interaction of the apt-TMP complex with nucleolin on the cellular surface and that the use of the AS1411 aptamer as a drug carrier may be a potential tactic in cancer therapy.

KEYWORDS: aptamer · nucleolin · 5,10,15,20-tetrakis(1-methylpyridinium-4-yl)porphyrin · photodynamic therapy

Aptamers are small, simple, and synthetic DNA or RNA oligonucleotides that can fold into a three-dimensional structure as a non-immunogenic alternative to bind to their target proteins specifically.[1] The AS1411 aptamer is based on a 26-base guanine-rich oligonucleotide which forms a dimeric G-quadruplex structure to target nucleolin with high affinity and specificity. It is stable in serum for at least 3 days.[2−6] The G-quadruplex structure is a specialized G-rich DNA structure that can be composed of four guanines (also known as G-quartet) by Hoogsteen hydrogen binding and stabilized by monovalent cations, such as potassium or sodium.[7] Several important G-rich genomic regions, including telomeres and promoters, were found to potentially form G-quadruplex structures and to play many important roles inside cells.[7−9]

Human nucleolin, a multifunctional protein involved in RNA transcription, DNA replication, rRNA process, and BCl-2 stabilization,[2,10,11] can act as a shuttle to transfer molecules between the cell surface and the nucleus.[12] It has been shown that several cancer cells with a higher proliferation rate, including breast cancer cells,[2] lymphocytic leukemia,[13] hepatocellular carcinomas,[14] prostate carcinoma, and renal cell carcinoma,[15] have a higher nucleolin expression than normal cells.[6] Moreover, nucleolin has been shown to bind to and internalize the heparin-binding growth factor midkine, the tumor-homing 34 amino acid peptide (F3), the iron-binding lycoprotein lactoferrin, and acharan sulfate.[12,16−18] The findings revealed that nucleolin may be a good candidate for targeting anticancer therapies by internalization of specific ligands. Since the AS1411 aptamer is a biocompatible and good selector for the higher nucleolin-expressing cancer cells, and because its G-quadruplex structure is constantly stable, it could be a good candidate for carrying a quadruplex ligand, such as 5,10,15,20-tetrakis(1-methylpyridinium-4-yl)porphyrin (TMPyP4).

TMPyP4 that was used in the study is one of the porphyrin derivatives and is broadly used in photodynamic therapy (PDT), which is one of the most promising and non-invasive methods for treating malignant or premalignant tissue. Applications of PDT in treating patients with breast,[19] prostate,[20] lung,[21] and esophageal[22,23] cancers are now well-performed by the use of an exogenous porphyrin as a photosensitizer. It can be excited by optima light to generate singlet oxygen in cancer lesions to rapidly react with any nearby biomolecules and to promote cell death.[10,24] In addition, TMPyP4 is a quadruplex ligand, and its aromatic and cationic properties let it

*Address correspondence to soloman@ntu.edu.tw.

Received for review October 7, 2009 and accepted February 6, 2010.

Published online February 18, 2010.
10.1021/nn901374b

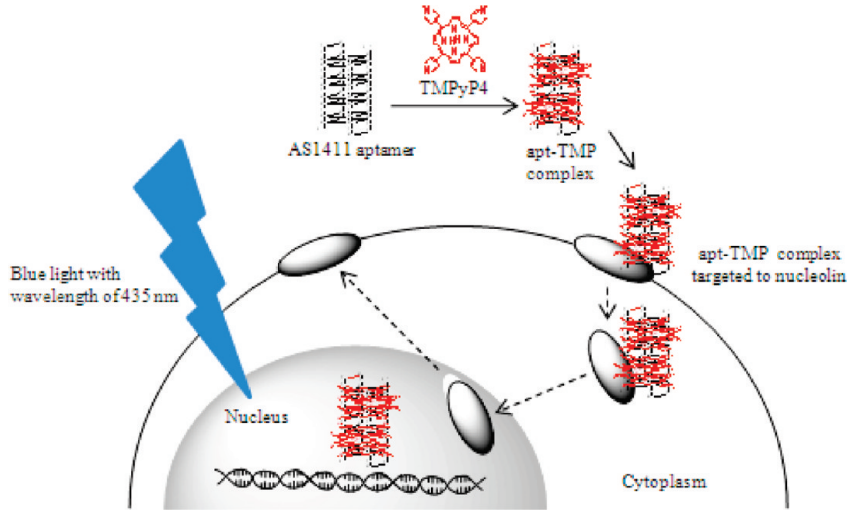

Figure 1. Structure and model for the mechanism of action of the apt-TMP complex. The apt-TMP complex was internalized after binding to nucleolin, which was expressed on the surface of tumor cells. When exposed to blue light, tumor cells with the apt-TMP complex uptake would be destroyed.

bind to and stabilize the G-quadruplex formation in human telomere, ranging in size from 3 to 15 kb tandem repeat of the sequence 5′-GGTTAG-3′, to inhibit the telomerase function, and to cause cellular senescence.[25−27] However, TMPyP4 is a poor selection and toxic to some of the normal cell lines, especially in normal fibroblast and epithelium while they are exposed to light.[28] Target delivery systems for TMPyP4 must be considered to increase their accumulation in the target site and to prevent toxicity at the neighboring tissues.

Herein, we use a selective and stable aptamer, the AS1411 aptamer, as a drug carrier to deliver a quadruplex ligand, TMPyP4, into the MCF7 breast cancer cell to create a higher TMPyP4 accumulation in the MCF7 cell compared to the normal epithelium cell (M10 cell). The target and delivery mechanism is based on the specific interaction of the aptamer-TMPyP4 complex (apt-TMP) with nucleolin that is overexpressed in breast cancer cells and the subsequent nucleolin-mediated internalization of apt-TMP. Bagalkot *et al.* have claimed that doxorubicin could form a physical complex with the aptamers through noncovalent intercalation, a process requiring no modification of doxorubicin or the aptamer, to maintain the safety and efficacy profile of the doxorubicin and the binding characteristics of the aptamer.[29] On the basis of this rationale, the resulting chemical modifications of TMPyP4 and the AS1411 aptamer may decrease the drug's efficiency and increase the failure of the G-quadruplex structure forming potential and specific target capability to the nucleolin. It would be desirable to develop simple but effective targeted TMPyP4 delivery strategies that do not require chemical modification of TMPyP4 drugs or the AS1411 aptamer. Herein, we hypothesize that the TMPyP4 molecules can be complexed to the AS1411 aptamer by the electrostatic attraction of the positively charged TMPyP4 and the negatively charged aptamer and then delivered into breast cancer cells to participate in further PDT even though TMPyP4 could not dissociate from the aptamer (Figure 1). The additional target specificity can be achieved by controlling the light irradiation to activate TMPyP4 to destroy the cancer cell.[30] Furthermore, the other advantage of this strategy is that TMPyP4 could release from the apt-TMP complex without breaking the covalent bond to target the telomeric DNA or DNA duplex of oncogene promoters to induce telomerase inhibition or to block oncogenne transcription when the complex entered the MCF7 cell nucleus by the nucleolin-mediated internalization.

RESULTS AND DISCUSSION

Herein, the different binding mode of TMPyP4 to the G-quadruplex structure is the first issue to be considered in the relevant studies, depending on the different DNA bases, ions, and pH values used in the fabrication process.[31−33] We first dissolved the AS1411 oligonucleotide in a salt solution, containing 200 mM KCl, 4 mM $MgCl_2$, and 28 mM Tris-HCl, annealed it at 100 °C for 5 min, and then slowly cooled it to room temperature to form the G-quadruplex structure, which is called the AS1411 aptamer. Then 4.5 μM TMPyP4 solution was titrated with the AS1411 aptamer solution, and the mixture solution was recorded by UV−vis spectrophotometry to study the interaction between TMPyP4 and the G-quadruplex of the aptamer.[34] Figure 2A shows the changes of intensity and location of the Soret band of TMPyP4 at the wavelength of 350 to 500 nm when titrated with the AS1411 aptamer. A red shift from 422 to 433 nm and an obvious hypochromicity of the Soret band (53%) was carried out while the AS1411 aptamer was continually added to the TMPyP4 solution. However, when free TMPyP4 drugs were fully

caught by the AS1411 aptamer, no difference of the Soret band could be detected even if more aptamers were added to the mixture solution. These results revealed that there was a red shift of the TMPyP4 Soret band in the intermediate level between the typical intercalated binding (15 nm) and the outside binding (8 nm) modes and a more obvious hypochromicity than that appearing in the intercalation binding mode (at least 35%).[35,36]

Since the Scatchard analysis is a practical tool to quantify the binding number of ligands to a receptor,[31,32] it can also be used to determine the binding ratio of TMPyP4 to the AS1411 aptamer. The Scatchard plot of r/C_f *versus* r from the titration data was constructed (Figure 2B), and the nonlinearity of the plot indicated the unequal binding constant, suggesting that there were multibinding modes and independent binding sites of TMPyP4 molecules with the G-quadruplex structure occurrence as recently reported.[35] By fitting with the Scatchard equation, data points at r values between 3.0 and 4.0 indicated that the TMPyP4 binding number n was 5.4 and the TMPyP4 binding constant K was 2.4×10^6; data points at r values between 4.0 and 6.5 indicated that the n was 7.3, and the K value was 1.06×10^7. These results revealed that the binding number of TMPyP4 per AS1411 aptamer was in the range of 5 to 7 when the apt-TMP complex was prepared in this condition. To ascertain more accurate numbers of TMPyP4 binding, the continuous variation analysis (Job plot) was used. The point of the intersection of two fitting lines in the Job plot for the prepared apt-TMP complex demonstrated that the mole fraction of TMPyP4 in the complex solution was 0.86, suggesting that one AS1411 aptamer molecule would bind with 6.1 TMPyP4 molecules (Figure 2C), which was in range with the TMPyP4 binding number obtained from the Scatchard plot fitting. These results suggested that a AS1411 aptamer/TMPyP4 molar ratio of 1/6 should form the most efficient complex and could be used for further investigation.

In order to confirm the G-quadruplex structure that could not be destroyed by the binding TMPyP4 to decrease the interaction of the aptamer with nucleolin and the internalization of the apt-TMP complex, the CD spectra can be analyzed after the completion of the TMPyP4 binding. The positive peak at 262 nm and the negative peak at 238 nm indicated that the G-quadruplex structure was still maintained (Figure 3A).[5] Moreover, the CD spectrum at the range of 400 to 500 nm can be used to determine and to establish the intercalary or outside binding of porphyrins to the G-quadruplex structure: a positive induced CD band is indicative of outside binding, and a negative induced CD band is representative of intercalation.[31,37] Therefore, as shown in Figure 3A, the evident oscillation CD signals appearing between 400 and 450 nm suggested that a mixed binding mode of TMPyP4 to the AS1411

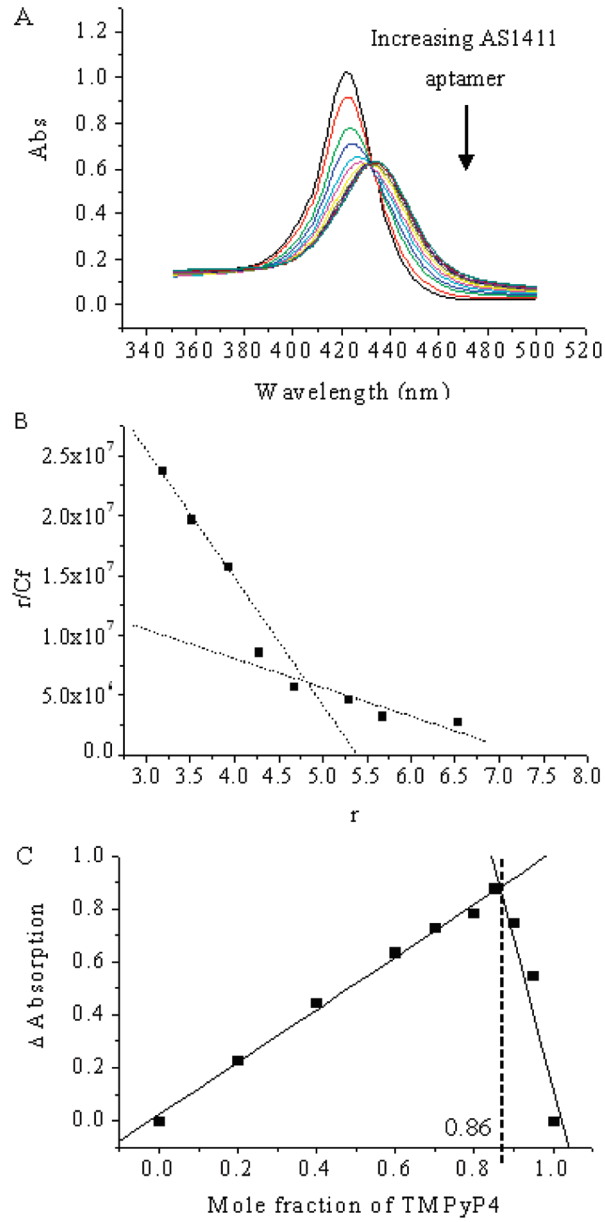

Figure 2. (A) UV−vis absorption titration spectra of 4.5 μM TMPyP4 with aptamer addition from 0 to 1.8 μM. (B) Scatchard plots for TMPyP4 with aptamer. (C) Job plots for the binding of TMPyP4 to the aptamer. The aptamer was in 200 mM KCl, 4 mM $MgCl_2$, and 28 mM Tris-HCl (pH = 8.0).

aptamer developed, resulting in a counteraction of the CD band magnitude and an unclear CD spectrum at the range of 400 to 500 nm. In order to verify the binding modes of TMPyP4 to the aptamer, the energy transfer experiment was also carried out by a fluorescence spectrophotometer in our study. Other researchers have demonstrated that, if a fluorescent ligand closely contacts the secondary structure of the DNA *via* intercalation, the energy will transfer from the DNA to the ligand after being excited with the DNA absorption and induce a strong enhancement of the emission intensity of the ligand. However, other modes of ligand binding such as end-pasting or the aggregation on the DNA surface give rise to a situation where the ligands are not

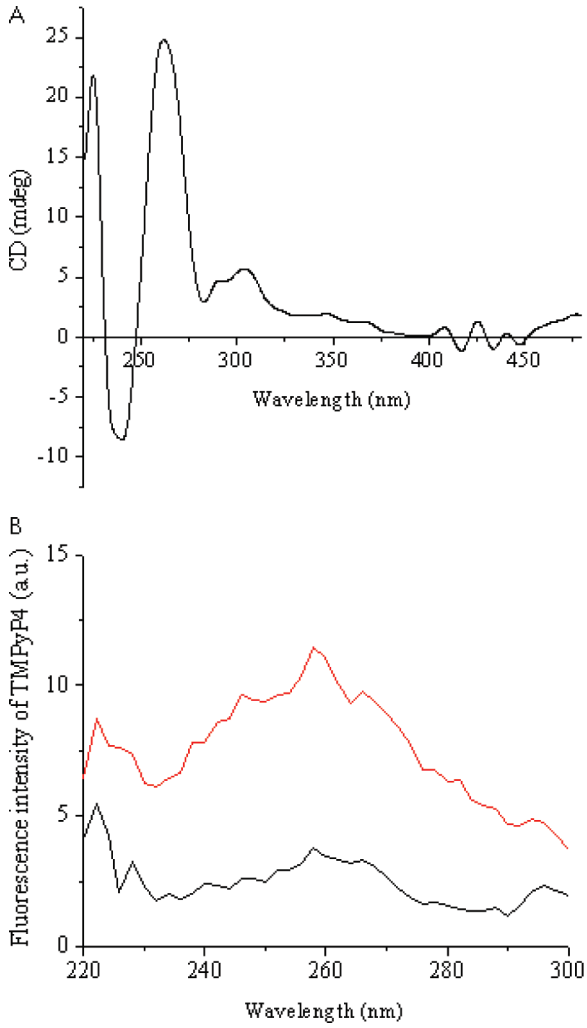

Figure 3. (A) Circular dichroism (CD) spectra of the apt-TMP complex. (B) Fluorescent energy transfer from the aptamer G-bases to TMPyP4. Excitation spectra (λ_{em} = 660 nm) of free TMPyP4 (black line) and the apt-TMP complex (red line) were recorded with a fluorescence spectrophotometer in a quartz cell (1 cm × 1 cm) with a band-pass of 5 nm at the excitation and emission side.

in close contact with the bases and are in an unfavorable orientation for energy transfer.[31,37,38] As seen in Figure 3B, the fluorescence emission of TMPyP4 solution at 660 nm was weak when excited between 220 and 350 nm, which was the DNA absorption region (black line). However, the emission intensity of TMPyP4 was strongly enhanced when binding with the AS1411 aptamer (red line) as a consequence of energy transfer from G-quartet to porphyrin residues. These data clearly showed that significant transfer of energy occurred from excited G-bases to TMPyP4, thus suggesting an intercalative mode of TMPyP4 binding to the AS1411 aptamer. The binding mechanism of the G-quadruplex−TMPyP4 complex has been studied by Haq *et al.* who indicated that TMPyP4 could recognize G-quadruplex aptamers and bond between two G-quartets shown in a space-fill mode and a relatively lower energy.[39] Besides, they also disclosed that TMPyP4 binding between two adjacent G-quartets was more favorable than either end-pasting or loop intercalation, where only a single G-quartet is implicated. Therefore, from the results shown in the CD spectrum and the fluorescence energy transfer study (Figure 3), four TMPyP4 molecules were assumed to intercalate into four groups of adjacent stacked G-quartets of the AS1411 aptamer, and the other two TMPyP4 molecules presented end-pasted arrangements. Moreover, the recognized TMPyP4 sequence not only exists in the AS1411 aptamer but also shares with other G-quadruplex aptamers, such as thrombin-binding aptamer, which had been investigated by del Toro *et al.*, who demonstrated that TMPyP4 bonded the G-quadruplex structure of the thrombin-binding aptamer *via* an intercalative binding mechanism.[40]

The transmission electron microscope (TEM) image (Figure 4A) shows the particle size distribution of the prepared apt-TMP complex. Mandelkern *et al.* have pointed out that one nucleotide unit is 3.3 Å (0.33 nm) long.[41] Therefore, the AS1411 with 13 nucleotide units in the length should have an ideal length of 4.3 nm theoretically. However, the apt-TMP complex in our study was shown to be in the range of 7 to 28 nm in the TEM micrograph, suggesting that the aggregation of the apt-TMP complexes might occur in this prepared condition. Figure 4B shows the stability of the prepared apt-TMP complex against degradation and digestion of DNase I, as seen by the use of nondenaturing polyacrylamide gel electrophoresis. When the AS1411 aptamer and the apt-TMP complex were treated with the enzyme DNase I, no obvious digested DNA bands could be observed on the gel. Conversely, for AT26, the 26 base pair oligonucleotides, without G-quadruplex structure formation, were completely digested and could not be observed on the gel. In addition, since the AS1411 aptamer based on a 26-base guanine-rich oligonucleotide folded into a compact structure, a dimeric G-quadruplex structure, it might migrate more easily and rapidly in 15% nondenaturing polyacrylamide gel than the linear forms of AT26 or DNA marker. In fact, there was no degradation of AS1411 aptamer demonstrated. The drag phenomenon of the AS1411 aptamer band was assumed to be due to the special G-quadruplex structure of AS1411 aptamer, and the similar phenomenon was also found by Han *et al.*, who used native gel electrophoresis to compare the possible differential effects of the three positional porphyrin isomers in facilitating the formation of parallel and antiparallel G-quadruplex structure.[42] The unclear DNA band appearing on the gel might be due to the fluorescence quenching of the FITC−AS1411 aptamer by TMPyP4. Since ethidium bromide could not intercalate easily into the AS1411 aptamer, in order to evaluate the G-quadruplex structure formation in the apt-TMP complex and the stability of the complex against DNase I

digestion, the fluorescein isothiocyanate conjugated AS1411 aptamer (FITC−AS1411 aptamer) was used to bind with TMPyP4 to form the apt-TMP complex (FITC−apt-TMP complex) and then treated with DNase I. The emission wavelength of FITC was about 518 nm, which was close to the absorption wavelength of the TMPyP4. Therefore, when FITC−apt-TMP complex or DNase I treated FITC−apt-TMP complex was run in 15% nondenaturing polyacrylamide gel and then placed on an ultraviolet transilluminator, the fluorescence of FITC was quenched as a result of TMPyP4 absorbance and resulted in a unclear DNA band. Furthermore, no DNA fragment smear could be detected on the gel after the FITC−AS1411 aptamer or FITC−apt-TMP complex was digested with DNase I. Therefore, both the FITC−AS1411 aptamer and FITC−apt-TMP complex were stable against DNase I digestion. The small size of the apt-TMP complex and the high stability against DNase I digestion may facilitate the apt-TMP complex with a rapid vascular extravasation and intratumoral penetration and high stability in blood, thereby making it a therapeutically effective drug delivery system for *in vivo* applications. Moreover, the lower release profile of TMPyP4 from the apt-TMP complex (Figure 4C) pointed out that the interaction between TMPyP4 and the AS1411 aptamer *via* intercalation and outside bound was strong and resulted in a low TMPyP4 release from the complex (only 26% at 120 h incubation time).

After confirming the TMPyP4 binding number, binding modes, particle size, and stability of the apt-TMP complex, the intracellular uptake of the pure TMPyP4 drug and the apt-TMP complex was estimated from the fluorescence intensities of MCF7 and M10 cells by a flow cytometry (Figure 5A). The results showed that the fluorescence intensity of internalization of TMPyP4 and the apt-TMP complex in MCF7 cells was 12.7 and 20.2%, respectively. In addition, the fluorescence intensity in M10 cells was 14.3 and 5.3% when fed with TMPyP4 and the apt-TMP complex for 2 h, respectively. Calculations showed that the amounts of internalization of the prepared apt-TMP complex in MCF7 breast cancer cells was 3.8 times higher than that in M10 normal cells, but M10 cells showed a slightly higher TMPyP4 internalization than MCF7 cells. In order to evaluate the role of nucleolin in the cellular uptake of the apt-TMP complex, the mixture of the prepared apt-TMP complex and free AS1411 aptamers or monoclonal nucleolin antibody MS-3 was fed to the MCF7 cells. Figure 5B shows that there was a 13.8% fluorescence intensity decrease when using the free AS1411 aptamer to compete with the apt-TMP complex to nucleolin expressed at the cell membrane. In addition, if using the monoclonal nucleolin antibody MS-3 as competitors against the prepared apt-TMP complex, the intensity of red fluorescence decreased from 15.7 to 5.3%. These results demonstrated that

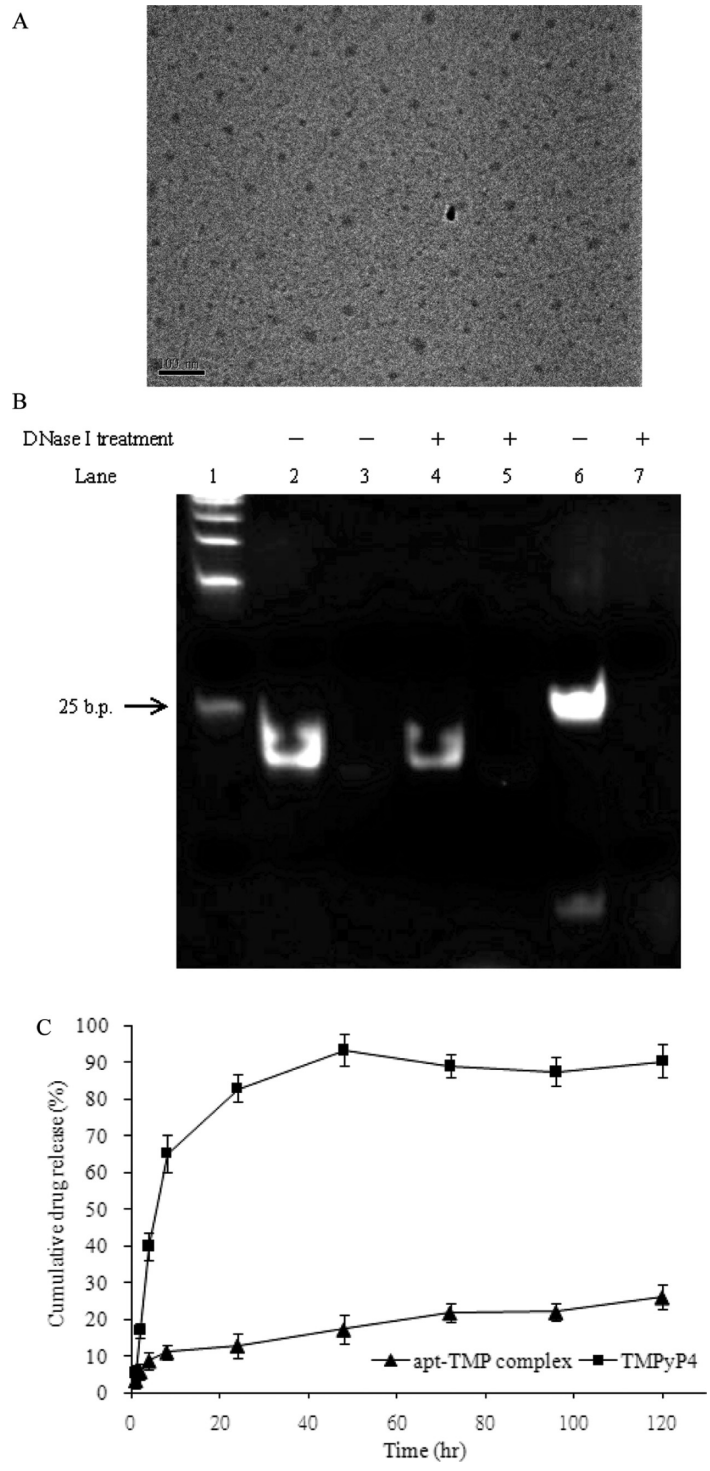

Figure 4. (A) TEM image of the prepared apt-TMP complex with a AS1411 aptamer/TMPyp4 molar ratio of 1/6. The scale bar is 100 nm. (B) Resistant digestion of the apt-TMP complex by DNase I. Lane 1, 25 bp marker; lane 2, FITC−AS1411 aptamer alone; lane 3, FITC−apt-TMP complex with a AS1411 aptamer/TMPyp4 molar ratio of 1/6; lane 4, FITC−AS1411 aptamer after treatment with 400U DNase I; lane 5, FITC−apt-TMP complex after treatment with 400U DNase I; lane 6, oligonucleotide AT26; and lane 7, oligonucleotide AT26 after treatment with 400U DNase I. (C) *In vitro* release profile of free TMPyP4 (shown in closed square) and the apt-TMP complex (shown in closed triangle).

the enhancement of cellular association and uptake was induced by the specific interaction of the apt-TMP complex with nucleolin at the cellular surface

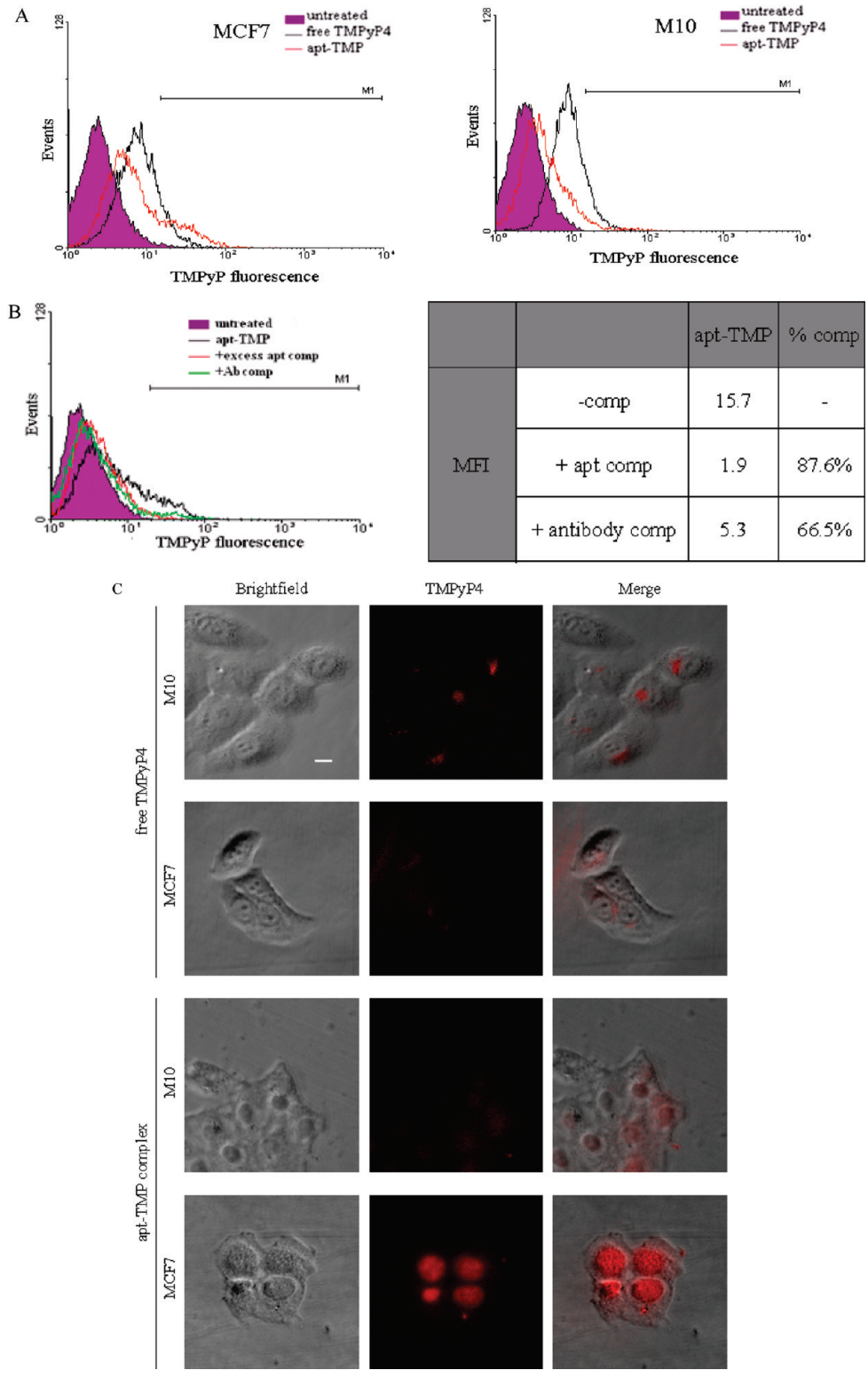

		apt-TMP	% comp
MFI	-comp	15.7	-
	+ apt comp	1.9	87.6%
	+ antibody comp	5.3	66.5%

Figure 5. Red fluorescence of TMPyP was assessed by flow cytometry. (A) Cell-type specific binding of the apt-TMP complex. Cell surface binding of free TMPyP4 (20 μM) (shown in black) or the apt-TMP complex (shown in red) was tested for binding to MCF7 and M10 cells. (B) MCF7 cells were incubated with the apt-TMP complex alone (black), co-cultured with 10-fold excess free AS1411 aptamer to compete with the apt-TMP complex (red), and incubated with 30 μg of monoclonal antibody MS-3 followed by adding the apt-TMP complex (green). Untreated cells are shown in purple. Uptake of TMPyP4 is displayed as % mean fluorescence intensity (MFI) in the M1 gate. MFI values ± competitor of the entire population of the indicated sample were used to calculate the % competition (listed in table). (C) Subcellular localization of free TMPyP4 (10 μM) and the apt-TMP complex after 2 h incubation with MCF7 and M10 cells. The enhancement of uptake was specific for MCF7 cells. Scale bar is 10 μm.

and by subsequent engulfment through the nucleolin-mediated internalization.

It has been reported that breast cancer cells show high-level nucleolin expression in comparison with normal cells,[2] and that nucleolin in the cell acts as a shuttle to transfer molecules between the cell surface and the nucleus. To determine the subcellular localization of apt-TMP in breast cancer and normal cells related with nucleolin expression, the red fluorescence of TMPyP4 in MCF7 and M10 cells could be observed under a fluorescence microscope after cells were fed with TMPyP4 or the apt-TMP complex for 2 h. The pure TMPyP4 drug could only be uptaken and distributed in the cytoplasm of MCF7 and M10 cells and then could be excited by a green laser to emit red light (Figure 5C). However, when TMPyP4 was complexed with the AS1411 aptamer and then fed to MCF7 and M10 cells, the large part of red fluorescence could be detected in the nuclei in either MCF7 or M10 cells, and the red fluorescent intensity in the nuclei of MCF7 cells was higher than that in the M10 cell nuclei. These results demonstrated that the TMPyP4 uptake in MCF7 cells could be enhanced by the interaction of the apt-TMP complex with nucleolin, and a high TMPyP4 molecules accumulation in MCF7 cell nucleus could then be utilized to target the telomeric DNA[35] or DNA duplex of oncogene promoters[34] to induce telomerase inhibition or to block oncogene transcription.[34,43]

Finally, we were interested in evaluating the specificity and phototoxicity of the apt-TMP complex as a photosensitizer delivery platform for PDT to breast cancer cells. Herein, MCF7 and M10 cells were incubated with the pure TMPyP4 drug and the apt-TMP complex for 2 h, washed twice with PBS, and then irradiated with a blue light (435 nm, 7.1 mW/cm^2) for a serial period to determine the light dose on cellular phototoxicity. After 24 h of reincubation in fresh medium, the cell viability was assayed by MTT assay (Figure 6A). In TMPyP4 treated or apt-TMP complex treated cells without light exposure, no cytotoxicity could be observed. However, when TMPyP4 treated or apt-TMP complex treated cells were irradiated, cell viability dramatically decreased according to the light exposure time either for MCF7 or M10 cells. Importantly, the phototoxicity of the apt-TMP complex in MCF7 cells was higher than that of free TMPyP4 for all irradiation times. In contrast, when M10 cells were treated with the apt-TMP complex and exposed to light, the cytotoxicity was lower than having been treated with free TMPyP4 drugs only. In the comparison of the cell viability between MCF7 and M10 after pure TMPyP4 drug treatment and then light exposure for 180 s (Figure 6B), there was a higher phototoxicity in M10 cells than in MCF7 cells. However, the phototoxicity of the apt-TMP complex in MCF7 cells was significantly higher than in M10 cells after irradiation of blue light for 180 s, and the phototoxicity of TMPyP4 in M10 cells could be reduced when the TMPyP4 drug was complexed with the AS1411 aptamer. The higher apt-TMP complex in MCF7 breast cancer cells resulted in a

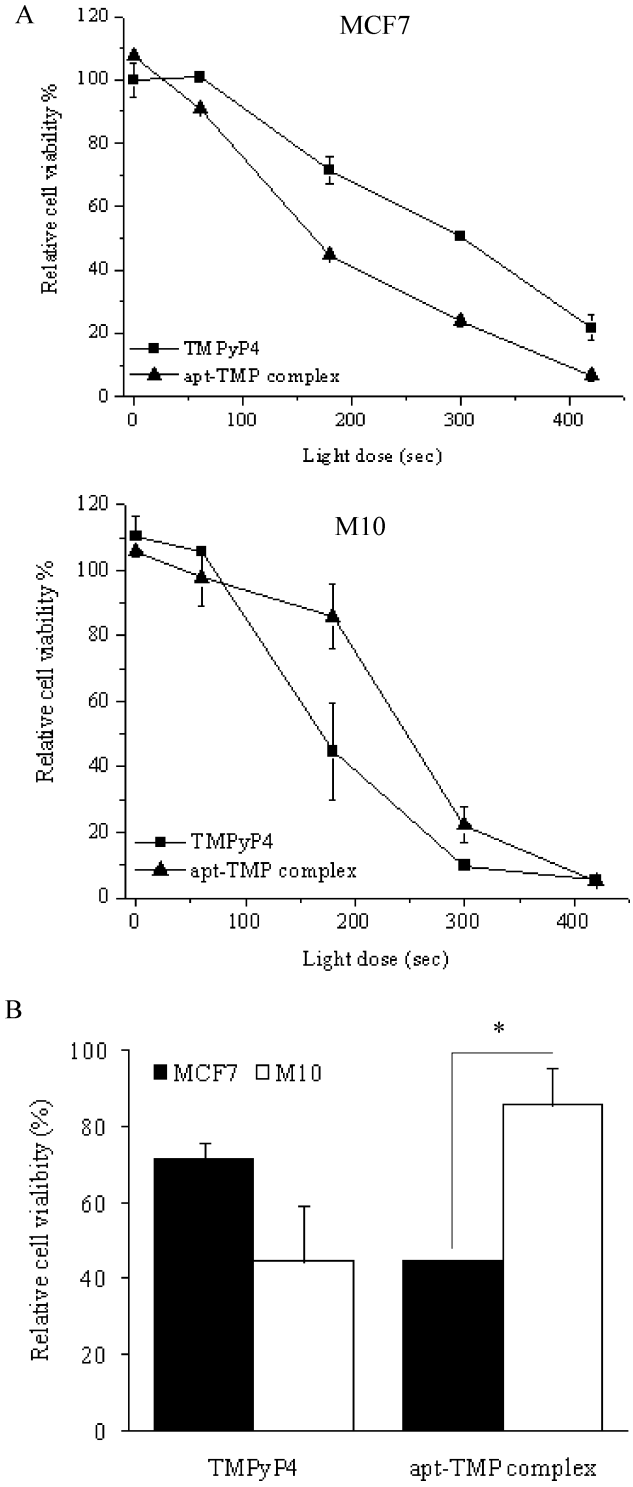

Figure 6. Cell-type specific photocytoxicity of the apt-TMP complex. (A) MCF7 and M10 cells were treated with free TMPyP4 drug and the prepared apt-TMP complex at a TMPyP4 concentration of 1 μM. Cells were further cultured for 2 h to allow the uptake of TMPyP4 and the apt-TMP complex. Cells were washed twice with PBS and then exposed to a blue light (435 nm, 7.1 mW/cm^2) for a serial period. Cells were further incubated for 24 h and determined by MTT assay. (B) Relative cell viability of MCF7 and M10 cells when fed with free TMPyP4 drug and the prepared apt-TMP complex at a TMPyP4 concentration of 1 μM for 2 h and then treated with the blue light for 180 s; *$p < 0.05$.

larger phototoxicity on MCF7 than on M10 cells, demonstrating that the nucleolin-mediated uptake of the apt-TMP complex rather than nonspecific simple diffusion either significantly reduced the side effects of the TMPyP4 drug in normal epithelium cells or improved the photodamage in cancer cells. By analyzing the entire population in MCF7 cell lines revealed in Figure 5A, it showed more cellular uptake of free TMPyP4 drugs than the apt-TMP complex, but the phototoxicity of the apt-TMP complex in MCF7 cells was higher than that of free TMPyP4 (Figure 6B). This discrepancy might be due to the location of TMPyP4 accumulation: free TMPyP4 drugs accumulated in the MCF7 cytoplasm; the apt-TMP complex accumulated in the MCF7 nucleus (Figure 5C). Besides, it was pointed out that PDT-induced cell apoptosis could be suppressed by natural antioxidants such as curcumin, α-tocopherol, and $^1O_2$ scavengers existing in cytoplasm.[44] Therefore, the phototoxicity induced by TMPyP4, which accumulated in the MCF7 cytoplasm, would be suppressed by these natural antioxidants. On the contrary, when the complex was fed to MCF7 cells and engulfed *via* the specific nucleolin-mediated internalization, the apt-TMP complex mostly accumulated in the MCF7 nucleus lack of antioxidants, and, consequently a significant PDT-induced cytotoxicity was achieved in our study.

CONCLUSIONS

In conclusion, herein we successfully fabricated the apt-TMP complex as a slow photosensitizer delivery system, and the characteristics analysis revealed that six molecules of TMPyP4 could be complexed tightly to a AS1411 aptamer *via* intercalation and outside binding while not destroying the G-quadruplex structure in the complex. *In vitro* studies showed that MCF7 cells with high nucleolin expression had a large apt-TMP complex uptake and serious photodamage in comparison to the normal epithelium cell. The G-quadruplex of the AS1411 aptamer appears to be an ideal vector for nucleolin targeting and breast cancer specific drug delivery.

METHODS

Materials: AS1411, based on the oligonucleotide sequence of 5′-(GGTGGTGGTGGTTGTGGTGGTGG TGG), 5′-FITC-AS1411, and AT26, with an oligonucleotide sequence of 5′-(AAAAAAAAAAAAATTTTTTTTTTTT) was purchased from Mission Biotech (Taipei, Taiwan) and used without further purification. Oligonucleotides were diluted in sterile water to generate a concentration of 400 μM and stored at −20 °C for follow-up study. Deoxyribonuclease I (DNase I, from bovine pancreas) was obtained from Sigma-Aldrich (St. Louis, MO). TMPyP4 was purchased from TCI America (Boston, MA). Anhydrous dimethyl sulfoxide (DMSO) was purchased from Riedel-de Haën (Germany). Disodium dihydrogen ethylenediamine tetraacetate dehydrate was purchased from SHOWA CHEMICAL Co., Ltd. (Tokyo, Japan). They were all at a reagent grade and used without further purification.

Synthesis and Characteristics of the apt-TMP Complex: The G-quadruplex structure of the AS1411 aptamer in a salt solution, containing 200 mM KCl, 4 mM $MgCl_2$, and 28 mM Tris-HCl, was formed by annealing it at 100 °C for 5 min and slowly cooling it to room temperature. Then, a 4.5 μM TMPyP4 solution was titrated with the AS1411 aptamer solution, and the mixture solution was recorded by UV−vis spectrophotometry (CARY 50 Conc, VARIAN; Australia) until no intensity and location shift change of the Soret band of TMPyP4 could be observed. The titration curve of TMPyP4 by AS1411 was plotted to get the Scatchard plot.[31,32] The Scatchard equation, $r/C_f = K(n - r)$, was used to calculate the binding affinity of TMPyP4 to AS1411 (K) and the binding number of TMPyP4 (n). The binding ratio r was defined as the concentration of bound TMPyP4 per mol AS1411 aptamer (*i.e.*, C_b/C_{apt}). $C_b = (A_f - A_{bn})/(\varepsilon_f - \varepsilon_b)$, where A_f and A_{bn} were the absorbance of the free TMPyP4 and any titration points decreased by the AS1411 aptamer at 424 nm. The value of ε_f and ε_b referred to the absorbance of the free and fully bound TMPyP4 divided to C_t, where C_t was the total concentration of TMPyP4. The concentration of free TMPyP4 (C_f) was calculated by $C_f = C_t - C_b$. The percentage of hypochromicity (H) of the Soret band of TMPyP4 could be calculated by using $H(\%) = [(\varepsilon_f - \varepsilon_b)/\varepsilon_f] \times 100$, where ε_f and ε_b were the extinction coefficient at the Soret band (422 nm).[32]

The continuous variation analysis was used to determine the Job plot[31] to obtain more accurate numbers of TMPyP4 binding per AS1411 aptamer. The examination process was done according to the method of Wei *et al.*[31] and is described as follows: By keeping the total concentration of the TMPyP4 and AS1411 aptamer at 6 μM in sterile water, the difference in UV−vis absorbance of the apt-TMP complex and the free TMPyP4 drug at 420 and 444 nm was recorded and calculated as the function of TMPyp4 fraction in the TMPyP4/AS1411 aptamer mixture solution to achieve the Job plot. Linear regression analysis was calculated with the software Origin 7.5.

In order to confirm the G-quadruplex structure that could not be destroyed by the binding TMPyP4 and to determine the binding mode of TMPyP4 to the AS1411 aptamer, the CD spectra and fluorescent energy transfer of the prepared apt-TMP complex were analyzed by a Jasco J-720 spectrometer (Jasco; Maryland) and a fluorescence spectrophotometer with a xenon flash lamp as a light source (CARY Eclipse, VARIAN), respectively. The CD spectra were recorded from 220 to 500 nm, and the recording specifications were a speed of 50 nm/min, response time 0.25 s, bandwidth 1.0 nm, and 2 times accumulation. A wavelength in the range of 220 to 320 nm was used to monitor the G-quadruplex formation in the AS1411 aptamer and the range of 350 to 500 nm to monitor the binding mode of TMPyP4 to the AS1411 aptamer. The fluorescence spectra were recorded in a 1 cm × 1 cm quartz cell with a band-pass of 5 nm at the excitation and emission side. The fluorescence spectrum of 1 μM of the free TMPyP4 drug was used to compare with the apt-TMP complex prepared at the AS1411 aptamer/TMPyP4 molar ratio of 1/6. The emission monochromator was set at 660 nm, and the excitation spectra were measured from 220 to 350 nm, the DNA absorption wavelength.

Transmission Electron Microscope Examination: Carbon-coated 200 mesh copper grids were immersed in the prepared apt-TMP complex solution with the AS1411 aptamer/TMPyP4 molar ratio of 1/6. Grids were placed on delicate-task-wipers to absorb excess liquid and then dried in a desiccator overnight. The dried copper grid with the apt-TMP complex was examined under the JEOL JEM-1230 transmission electron microscope (JEOL Co. Ltd.; JAPAN).

Stability of the apt-TMP Complex against DNase I Digestion and TMPyP4 Release from the apt-TMP Complex: The FITC-labeled AS1411 aptamer and FITC-labeled apt-TMP complex with a AS1411 aptamer/TMPyP4 molar ratio of 1/6 were prepared and treated with 400U DNase I at 37 °C for 30 min, followed by 10 mM EDTA inactivation. Oligonucleotide AT26 was used as a comparison to evaluate the protection of the G-quadruplex structure of the AS1411 aptamer against enzyme digestion. The enzyme treated aptamer and complex were then run on 15% nondenaturing polyacryla-

mide gel at 150 V for 45 min. The gel was stained with ethidium bromide (0.5 mg/mL) or the labeled FITC was directly photographed by using the UVP GDS-7900 imaging system (UVP Inc., Upland, CA).

To determine the release profile of TMPyP4 from the aptamer, the free TMPyP4 drug and the prepared apt-TMP complex suspended in 1 mL of phosphate buffered saline (PBS, pH 7.4) were placed in a Spectra/Por 1 dialysis tubing (SPECTRUM, Spectrum Laboratories Inc., CA) for the cutoff of 6−8 kDa molecules. The Spectra/Por 1 dialysis tubing was soaked in 500 mL of PBS as a dialytic buffer and gently shaken at 50 rpm at 37 °C. After shaking for a period of time, 3 mL of dialytic buffer was taken out to measure the TMPyP4 concentration by a fluorescence spectrometer at an excitation wavelength of 420 nm and an emission wavelength of 660 nm and then poured back to the drug release system. The amount of TMPyP4 released in each time interval was expressed as accumulation percentage of the total TMPyP4 bound to the AS1411 aptamer.

Measurement of the apt-TMP Complex Uptake: The human breast cancer cell line (MCF7) was originally obtained from the American Type Culture Collection (Rockville, MD). The normal human breast epithelium cell line (M10) was obtained from the Biosource Collection and Research Center, the Food Industry Research and Development Institute (Hsinchu, Taiwan). MCF7 and M10 cell lines were cultured in minimum essential medium (GIBCO; Grand Island, NY) supplement with 10% (v/v) fetal bovine serum, 100 IU/mL penicillin, 100 μg/mL streptomycin, and 250 ng/mL amphotericin, at 37 °C and in an atmosphere of 5% CO_2. The culture medium was changed on alternate days until confluence.

The following quantities of cells were seeded onto 12-well culture plates: 5×10^4/well MCF7 and 5×10^4/well M10. After the cell lines were cultured for 24 h, the medium was replaced with fresh medium containing the free TMPyP4 drug and the prepared apt-TMP complex at a TMPyP4 concentration of 20 μM. Cells were further cultured for 2 h to allow the uptake of the TMPyP4 and the apt-TMP complex. To determine the effect of aptamer/nucleolin-mediated internalization on the uptake of the apt-TMP complex, fresh culture media suspended with free AS1411 aptamer or monoclonal nucleolin antibody MS-3 (Santa Cruz Biotechnology; CA) were tested at the same time. The concentration of the free AS1411 aptamer (35 μM) or monoclonal nucleolin antibody MS-3 (30 μg) that was used was expected to result in a complete saturation with nucleolin expressing on the cell surface. After removal of the cultured medium, plates were washed with PBS three times and the cells were removed from the wells by using trypsin-EDTA, transferred to tubes, replaced the trypsin-contained medium with phosphate buffered saline (PBS), and then analyzed directly by a flow cytometry (EPICS XL Flow cytometry systems) to evaluate the apt-TMP uptake.

MCF7 and M10 cells suspended in culture medium were seeded onto 96-well plates. After the cell lines were cultured for 24 h, the medium was replaced with fresh medium containing the free TMPyP4 drug and the prepared apt-TMP complex at a TMPyP4 concentration of 10 μM. Cells were further cultured for 2 h to allow the uptake of TMPyP4 and the apt-TMP complex. Cells were then washed twice with PBS and replaced with fresh medium. Fluorescent images of the treated cells were obtained by a Zeiss Axiovert 200 M fluorescence microscope (Carl Zeiss Inc., Germany).

Phototoxicity of the apt-TMP Complex on the *In Vitro* Systems: The 5×10^3/well MCF7 and 5×10^3/well M10 cells that were suspended in culture medium were seeded onto 96-well plates and further cultured for 24 h. The medium was replaced with fresh medium containing the free TMPyP4 drug and the prepared apt-TMP complex at a TMPyP4 concentration of 1 μM. Cells were further cultured for 2 h to allow the uptake of TMPyP4 and the apt-TMP complex. Cells were washed twice with PBS and then exposed to blue light equipment (PCI Biotech AS, Norway Lumisource) at a wavelength of 435 nm and a fluence rate of 7.1 mW/cm^2. In order to evaluate the light dose on cellular phototoxicity, the TMPyP4 or apt-TMP complex treated cells were illuminated for a serial period. After light treatment, cells were reincubated in fresh medium for 24 h. The culture medium was replaced by 100 μL fresh medium containing 0.5 mg/mL 3-[4,5-dimethylthiazol-2-yl]-2,5-diphenyl tetrazolium bromide assays reagent (MTT assay, Alfa Aesar, San Francisco, CA), and then incubated at 37 °C for 3 h. Then, the MTT containing medium was added with 100 μL of acid/isopropanol solution, in which the concentration of HCl was 0.04 M to dissolve the MTT product, formazan. Finally, the absorbance was measured at 570 nm by ELISA reader (Sunrise-Basic Tecan, Switzerland). Viability of non-light-treated control cells was arbitrarily defined as 100%.

Statistical Analysis: All experiments were repeated and measured in triplicate. Results were reported as means ± SD, unless otherwise noted. Statistical significance was determined by using one-way analysis of variance (ANOVA). All *p* values were two-sided, and their significance level was 0.05. The software Statistical Package for Social Science 11.0 (SPSS 11.0) was used to conduct all statistical analyses.

Acknowledgment. This research was funded by National Science Council, ROC (NSC 96-2221-E-002-254-MY3).

REFERENCES AND NOTES

1. Nimjee, S. M.; Rusconi, C. P.; Sullenger, B. A. Aptamers: an Emerging Class of Therapeutics. *Annu. Rev. Med.* **2005**, *56*, 555–583.
2. Soundararajan, S.; Chen, W.; Spicer, E. K.; Courtenay-Luck, N.; Fernandes, D. J. The Nucleolin Targeting Aptamer AS1411 Destabilizes Bcl-2 Messenger RNA in Human Breast Cancer Cells. *Cancer Res.* **2008**, *68*, 2358–2365.
3. Dapić, V.; Bates, P. J.; Trent, J. O.; Rodger, A.; Thomas, S. D.; Miller, D. M. Antiproliferative Activity of G-Quartet-Forming Oligonucleotides with Backbone and Sugar Modifications. *Biochemistry* **2002**, *41*, 3676–3685.
4. Bates, P. J.; Kahlon, J. B.; Thomas, S. D.; Trent, J. O.; Miller, D. M. Antiproliferative Activity of G-Rich Oligonucleotides Correlates with Protein Binding. *J. Biol. Chem.* **1999**, *274*, 26369–26377.
5. Dapić, V.; Abdomerović, V.; Marrington, R.; Peberdy, J.; Rodger, A.; Trent, J. O.; Bates, P. J. Biophysical and Biological Properties of Quadruplex Oligodeoxyribonucleotides. *Nucleic Acids Res.* **2003**, *31*, 2097–2107.
6. Girvan, A. C.; Teng, Y.; Casson, L. K.; Thomas, S. D.; Jüliger, S.; Ball, M. W.; Klein, J. B.; Pierce, W. M., Jr.; Barve, S. S.; Bates, P. J. AGRO100 Inhibits Activation of Nuclear Factor-kappaB (NF-kappaB) by Forming a Complex with NF-kappaB Essential Modulator (NEMO) and Nucleolin. *Mol. Cancer Ther.* **2006**, *5*, 1790–1799.
7. Sen, D.; Gilbert, W. Formation of Parallel Four-Stranded Complexes by Guanine-Rich Motifs in DNA and Its Implications for Meiosis. *Nature* **1988**, *334*, 364–366.
8. Ambrus, A.; Chen, D.; Dai, J.; Bialis, T.; Jones, R. A.; Yang, D. Human Telomeric Sequence Forms a Hybrid-Type Intramolecular G-Quadruplex Structure with Mixed Parallel/Antiparallel Strands in Potassium Solution. *Nucleic Acids Res.* **2006**, *34*, 2723–2735.
9. Evans, T.; Schon, E.; Gora-Maslak, G.; Patterson, J; Efstratiadis, A. S1-Hypersensitive Sites in Eukaryotic Promoter Regions. *Nucleic Acids Res.* **1984**, *12*, 8043–8058.
10. Mongelard, F.; Bouvet, P. Nucleolin: a MultiFACeTed Protein. *Trends. Cell Biol.* **2007**, *17*, 80–86.
11. Ireson, C. R.; Kelland, L. R. Discovery and Development of Anticancer Aptamers. *Mol. Cancer Ther.* **2006**, *5*, 2957–2962.
12. Said, E. A.; Krust, B.; Nisole, S.; Svab, J.; Briand, J. P.; Hovanessian, A. G. The Anti-HIV Cytokine Midkine Binds the Cell Surface-Expressed Nucleolin as a Low Affinity Receptor. *J. Biol. Chem.* **2002**, *277*, 37492–37502.
13. Otake, Y.; Soundararajan, S.; Sengupta, T. K.; Kio, E. A.; Smith, J. C; Pineda-Roman, M.; Stuart, R. K.; Spicer, E. K.; Fernandes, D. J. Overexpression of Nucleolin in Chronic Lymphocytic Leukemia Cells Induces Stabilization of bcl2 mRNA. *Blood* **2007**, *109*, 3069–3075.
14. Trerè, D.; Derenzini, M.; Sirri, V.; Montanaro, L.; Grigioni, W.; Faa, G.; Columbano, G. M.; Columbano, A. Qualitative and Quantitative Analysis of AgNOR Proteins in Chemically

Induced Rat Liver Carcinogenesis. *Hepatology* **1996**, *24*, 1269–1273.
15. Pich, A.; Chiusa, L.; Margaria, E. Prognostic Relevance of AgNORs in Tumor Pathology. *Micron* **2000**, *31*, 133–141.
16. Christian, S.; Pilch, J.; Akerman, M. E.; Porkka, K.; Laakkonen, P.; Ruoslahti, E. Nucleolin Expressed at the Cell Surface is a Marker of Endothelial Cells in Angiogenic Blood Vessels. *J. Cell Biol.* **2003**, *163*, 871–878.
17. Legrand, D.; Vigié, K.; Said, E. A.; Elass, E.; Masson, M.; Slomianny, M. C.; Carpentier, M.; Briand, J. P.; Mazurier, J.; Hovanessian, A. G. Surface Nucleolin Participates in Both the Binding and Endocytosis of Lactoferrin in Target Cells. *Eur. J. Biochem.* **2004**, *271*, 303–317.
18. Joo, E. J.; ten Dam, G. B.; van Kuppevelt, T. H.; Toida, T.; Linhardt, R. J.; Kim, Y. S. Nucleolin: Acharan Sulfate-Binding Protein on the Surface of Cancer Cells. *Glycobiology* **2005**, *15*, 1–9.
19. Cuenca, R. E.; Allison, R. R.; Sibata, C.; Downie, G. H. Breast Cancer with Chest Wall Progression: Treatment with Photodynamic Therapy. *Ann. Surg. Oncol.* **2004**, *11*, 322–327.
20. Du, K. L.; Mick, R.; Busch, T. M.; Zhu, T. C.; Finlay, J. C.; Yu, G.; Yodh, A. G.; Malkowicz, S. B.; Smith, D.; Whittington, R.; Stripp, D.; Hahn, S. M. Preliminary Results of Interstitial Motexafin Lutetium-Mediated PDT for Prostate Cancer. *Lasers Surg. Med.* **2006**, *38*, 427–434.
21. Moghissi, K.; Dixon, K.; Thorpe, J. A.; Stringer, M.; Oxtoby, C. Photodynamic Therapy (PDT) in Early Central Lung Cancer: A Treatment Option for Patients Ineligible for Surgical Resection. *Thorax* **2007**, *62*, 391–395.
22. Ackroyd, R.; Kelty, C. J.; Brown, N. J.; Stephenson, T. J.; Stoddard, C. J.; Reed, M. W. Eradication of Dysplastic Barrett's Oesophagus Using Photodynamic Therapy: Long-Term Follow-Up. *Endoscopy* **2003**, *35*, 496–501.
23. Moghissi, K.; Dixon, K.; Thorpe, J. A.; Stringer, M.; Moore, P. J. The Role of Photodynamic Therapy (PDT) in Inoperable Oesophageal Cancer. *Eur. J. Cardiothorac. Surg.* **2000**, *17*, 95–100.
24. Oleinick, N. L.; Morris, R. L.; Belichenko, I. The Role of Apoptosis in Response to Photodynamic Therapy: What, Where, Why, and How. *Photochem. Photobiol. Sci.* **2002**, *1*, 1–21.
25. De Cian, A.; Lacroix, L.; Douarre, C.; Temime-Smaali, N.; Trentesaux, C.; Riou, J. F.; Mergny, J. L. Targeting Telomeres and Telomerase. *Biochimie* **2008**, *90*, 131–155.
26. Granotier, C.; Pennarun, G.; Riou, L.; Hoffschir, F.; Gauthier, L. R.; De Cian, A.; Gomez, D.; Mandine, E.; Riou, J. F.; Mergny, J. L.; Mailliet, P.; Dutrillaux, B.; Boussin, F. D. Preferential Binding of a G-Quadruplex Ligand to Human Chromosome Ends. *Nucleic Acids Res.* **2005**, *33*, 4182–4190.
27. Zahler, A. M.; Williamson, J. R.; Cech, T. R.; Prescott, D. M. Inhibition of Telomerase by G-Quartet DNA Structures. *Nature* **1991**, *350*, 718–720.
28. Rha, S. Y.; Izbicka, E.; Lawrence, R.; Davidson, K.; Sun, D.; Moyer, M. P.; Roodman, G. D.; Hurley, L.; Von Hoff, D. Effect of Telomere and Telomerase Interactive Agents on Human Tumor and Normal Cell Lines. *Clin. Cancer Res.* **2000**, *6*, 987–993.
29. Bagalkot, V.; Farokhzad, O. C.; Langer, R.; Jon, S. An Aptamer-Doxorubicin Physical Conjugate as a Novel Targeted Drug-Delivery Platform. *Angew. Chem., Int. Ed.* **2006**, *45*, 8149–8152.
30. Dolmans, D. E.; Fukumura, D.; Jain, R. K. Photodynamic Therapy for Cancer. *Nat. Rev. Cancer* **2003**, *3*, 380–387.
31. Anantha, N. V.; Azam, M.; Sheardy, R. D. Porphyrin Binding to Quadrupled T4G4. *Biochemistry* **1998**, *37*, 2709–2714.
32. Pasternack, R. F.; Gibbs, E. J. Porphyrin and Metalloporphyrin Interactions with Nucleic Acids. *Met. Ions Biol. Syst.* **1996**, *33*, 367–397.
33. Zhang, H. J.; Wang, X. F.; Wang, P.; Ai, X. C.; Zhang, J. P. Spectroscopic Study on the Binding of a Cationic Porphyrin to DNA G-Quadruplex under Different K^+ Concentrations. *Photochem. Photobiol. Sci.* **2008**, *7*, 948–955.
34. Ou, T. M.; Lu, Y. J.; Tan, J. H.; Huang, Z. S.; Wong, K. Y.; Gu, L. Q. G-Quadruplexes: Targets in Anticancer Drug Design. *ChemMedChem.* **2008**, *3*, 690–713.
35. Wei, C.; Jia, G.; Yuan, J.; Feng, Z.; Li, C. A Spectroscopic Study on the Interactions of Porphyrin with G-Quadruplex DNAs. *Biochemistry* **2006**, *45*, 6681–6691.
36. Pasternack, R. F.; Gibbs, E. J.; Villafranca, J. J. Interactions of Porphyrins with Nucleic Acids. *Biochemistry* **1983**, *22*, 2406–2414.
37. Lubitz, I.; Borovok, N.; Kotlyar, A. Interaction of Monomolecular G4-DNA Nanowires with TMPyP: Evidence for Intercalation. *Biochemistry* **2007**, *46*, 12925–12929.
38. Mergny, J. L.; Duval-Valentin, G.; Nguyen, C. H.; Perrouault, L.; Faucon, B.; Rougée, M.; Montenay-Garestier, T.; Bisagni, E.; Hélène, C. Triple Helix-Specific Ligands. *Science* **1992**, *256*, 1681–1684.
39. Haq, I; Trent, J. O.; Chowdhry, B. Z.; Jenkins, T. C. Intercalative G-Tetraplex Stabilization of Telomeric DNA by a Cationic Porphyrin. *J. Am. Chem. Soc.* **1999**, *121*, 1768–1779.
40. del Toro, M.; Gargallo, R.; Eritja, R.; Jaumot, J. Study of the Interaction between the G-Quadruplex-Forming Thrombin-Binding Aptamer and the Porphyrin 5,10,15,20-Tetrakis-(*N*-methyl-4-pyridyl)-21,23*H*-porphyrin Tetratosylate. *Anal. Biochem.* **2008**, *379*, 8–15.
41. Mandelkern, M.; *et al.* The Dimensions of DNA in Solution. *J. Mol. Biol.* **1981**, *152*, 153–161.
42. Han, H.; Langley, D. R.; Rangan, A.; Hurley, L. H. Selective Interactions of Cationic Porphyrins with G-Quadruplex Structures. *J. Am. Chem. Soc.* **2001**, *123*, 8902–8913.
43. Bates, P.; Mergny, J. L.; Yang, D. Quartets in G-Major. The First International Meeting on Quadruplex DNA. *EMBO Rep.* **2007**, *8*, 1003–1010.
44. Ryter, S. W.; Kim, H. P.; Hoetzel, A.; Park, J. W.; Nakahira, K.; Wang, X.; Choi, A. M. Mechanisms of Cell Death in Oxidative Stress. *Antioxid. Redox Signaling* **2007**, *9*, 49–89.